Proc. Natl. Acad. Sci. USA
Vol. 89, pp. 7625–7629, August 1992
Neurobiology

Neurally evoked calcium transients in terminal Schwann cells at the neuromuscular junction

(glial physiology/confocal microscopy/fluo-3/electron microscopy)

NOREEN E. REIST* AND STEPHEN J. SMITH

Department of Molecular and Cellular Physiology, Stanford University School of Medicine, Stanford, CA 94305-5426

Communicated by Robert Galambos, May 20, 1992

ABSTRACT **We examined the effects of motor-nerve stimulation on the intracellular Ca^{2+} levels of Schwann cells, the glial cells at the frog neuromuscular junction. Schwann cells, which were loaded with the fluorescent Ca^{2+} indicator fluo-3 and examined by confocal microscopy, showed a transient increase in free Ca^{2+} within a few seconds of the onset of tetanic stimulation of the motor nerve. The Ca^{2+} response was specific to the synapse in that it was found in the terminal Schwann cells at the junction but not in the myelinating Schwann cells along the axon. The Ca^{2+} transients occurred in the presence of *d*-tubocurare, indicating that they were not mediated by nicotinic acetylcholine receptors and recurred when the stimulus was repeated. The Ca^{2+} response persisted after degeneration of the postsynaptic muscle fiber, demonstrating that the terminal Schwann cell was stimulated directly by presynaptic activity. The finding that terminal Schwann cells at the neuromuscular junction respond to presynaptic activity suggests that glial-cell function is modulated by synaptic transmission.**

At a chemical synapse, activity in the presynaptic cell causes the release of a neurotransmitter that diffuses across an extracellular gap and generates a response in the postsynaptic cell (1). Glial cells, which are intimately associated with the presynaptic neuron, have been considered passive support cells uninvolved in synaptic transmission because they do not conduct action potentials. Recent studies demonstrating the presence of voltage-gated ion channels and neurotransmitter receptors in glial cells (for review, see ref. 2) have raised the possibility that these cells may be more than passive bystanders. The most direct evidence to date that glial cells are activated by synaptic transmission has been reported by Dani *et al.* (3), who have shown that stimulation of neural afferents can trigger actively propagating waves of intracellular Ca^{2+} through networks of astrocytes in cultured hippocampal slices.

Here we examine Ca^{2+} fluctuations within terminal Schwann cells, the glial cell at vertebrate neuromuscular junctions. At the frog neuromuscular junction, the nerve terminal arborizes into long, finger-like projections that form synaptic contacts in shallow gutters on the muscle surface. A thin process of terminal Schwann cell tightly caps the entire length of the nerve terminal and has periodic projections that extend around the terminal into the synaptic cleft (4). Along most of the length of the terminal arborization, this thin layer of terminal Schwann cell (0.06–0.3 μm, data not shown) is indistinguishable from the nerve terminal by light microscopy. However, at the level of the Schwann cell soma, the nerve terminal remains, on average, 1–2 μm across, while the Schwann cell widens to 4–8 μm across and, thus, is easily identifiable by using Nomarski (4) or fluorescence optics.

Our studies were done on the cutaneous pectoris muscle of the frog, where it is possible to remove the postsynaptic muscle fibers while leaving the presynaptic-nerve terminals and their Schwann cells intact (5). Thus, we could study the interactions between the nerve terminal and the Schwann cell independent of the muscle. Using this preparation, we were able to elicit Ca^{2+} transients within terminal Schwann cells by electrical stimulation of the motor nerve. We confirmed these results at intact neuromuscular junctions where Jahromi *et al.* (6) have recently reported similar findings. Here we demonstrate that terminal Schwann cells in acutely isolated tissue directly respond to neuronal activity and that this response is independent of the postsynaptic muscle.

MATERIALS AND METHODS

Intact Muscles. Observations were made at neuromuscular junctions of acutely isolated cutaneous pectoris muscles from adult male frogs, *Rana pipiens*.

Innervated Sheaths. Most experiments were conducted on a specialized presynaptic preparation of the frog neuromuscular junction. The cutaneous pectoris muscle was surgically damaged according to the procedures of Yao (5). Briefly, the muscle was exposed in the chest region of an anesthetized frog and viewed under a dissecting microscope so that the axonal arborization pattern was visible. Extrajunctional regions of the muscle were removed by cutting within 0.5–1 mm of the axonal branches without damaging the fine nerve processes. This procedure causes complete degeneration of the muscle fibers, thereby producing an innervated basal lamina sheath that consists of the nerve terminals, their terminal Schwann cells, and the basal lamina in the synaptic region. Regeneration of muscle fibers was prevented by x-irradiating frogs with a Philips 250-kV 15-mA x-ray unit [0.35-mm Cu filter, total dose per day equaled 3900 rads (1 rad = 0.01 Gy)] for 3–5 days after surgical damage. Degeneration of muscle fibers was generally complete within 2–3 weeks; preparations were used 3–8 weeks after damage. Some innervated sheaths exhibited regeneration of a few muscle fibers. For these preparations and for intact neuromuscular junctions, 10×10^{-6} M *d*-tubocurare was added to the Ringer's solution during stimulation trials to eliminate movement artifacts.

The nerve terminals and Schwann cells in these innervated sheaths have normal structure, as determined by scanning and transmission electron microscopy (5). In addition, the nerve terminals are functional, in that tetanic stimulation of the motor nerve increases intracellular Ca^{2+} (see Fig. 1), as seen at intact neuromuscular junctions. The advantages of this preparation are as follows: (*i*) it is very thin, thus allowing simultaneous examination of several terminal arborizations and their associated Schwann cells; (*ii*) it exhibits no mechanical distortion and minimal background fluorescence due to the lack of muscle fibers; and (*iii*) it allows examination of interactions between the nerve terminal and the terminal

The publication costs of this article were defrayed in part by page charge payment. This article must therefore be hereby marked "*advertisement*" in accordance with 18 U.S.C. §1734 solely to indicate this fact.

*To whom reprint requests should be addressed.

Schwann cells in the absence of any postsynaptic effects from the muscle.

Loading with Fluo-3 AM. Intact muscles or innervated sheaths were dissected from the frog along with ≥1 cm of motor nerve in frog Ringer's solution [115 mM NaCl/2.5 mM KCl/1.8 mM $CaCl_2$/2.61 mM Tris·HCl/0.38 mM Tris base (7)]. These tissues were then incubated for 2 hr at 26°C in 100 μM fluo-3 AM (Molecular Probes) in Ringer's solution/2.5% dimethyl sulfoxide/0.2% pluronic F-127 (Molecular Probes) and were washed 15 min–1 hr in Ringer's solution.

Image Acquisition. Images were acquired at a rate of one frame every 2 sec by using a modified Bio-Rad MRC-500 confocal laser microscope (488-nm excitation wavelength) equipped with an Olympus DApo40UV objective lens (numerical aperature, 1.3). Images were recorded by using a Panasonic TQ-2028F optical memory disc recorder. After recording a baseline of 30–40 sec in the resting state, the motor nerve was stimulated electrically at 50 Hz (1 msec, 0.5 mA; WPI Isostim A320) for 10–20 sec with a suction electrode.

Image Processing. To improve the signal/noise ratio in static fluorescence micrographs, three to five consecutive frames were averaged. To examine the change in fluorescence of given structures over time, rectangular subareas were selected, the average fluorescence value of each area was calculated in each frame, and the mean background (calculated in an area devoid of cells—for example, Fig. 1*C*, box 4) was subtracted. For Fig. 1*D*, these data were plotted directly vs. time. In Figs. 2–4, these data are expressed as a ratio of fluorescence intensity to mean resting fluorescence (F/F_0). The mean resting fluorescence of a given structure was defined as the mean fluorescence of the subarea averaged over 15–20 frames immediately before each stimulation.

Electron Microscopy. Tissue was processed for electron microscopy, as described (8). Briefly, muscles were fixed for 30 min in 1% glutaraldehyde/0.09 M phosphate buffer, postfixed for 1 hr in 1% osmium tetroxide in buffer, dehydrated for 30 min in ethanol, soaked for 15 min in propylene oxide, embedded overnight in an Epon/Araldite mixture, sandwiched between glass slides, and baked for 1 hr at 90°C. This procedure provided a thin (<1 mm) wafer of plastic-embedded tissue. Previously identified Schwann cells were easily relocated in the whole-mount preparation by following the procedures of McMahan *et al.* (4), and that region was then cut out and mounted for sectioning. Semithin sections (1 μm) were stained with 1% toluidine blue; thin sections (70 nm) were stained with uranyl acetate and lead citrate.

RESULTS

Stimulation of the motor nerve caused a transient increase in intracellular Ca^{2+} in terminal Schwann cells. An example of

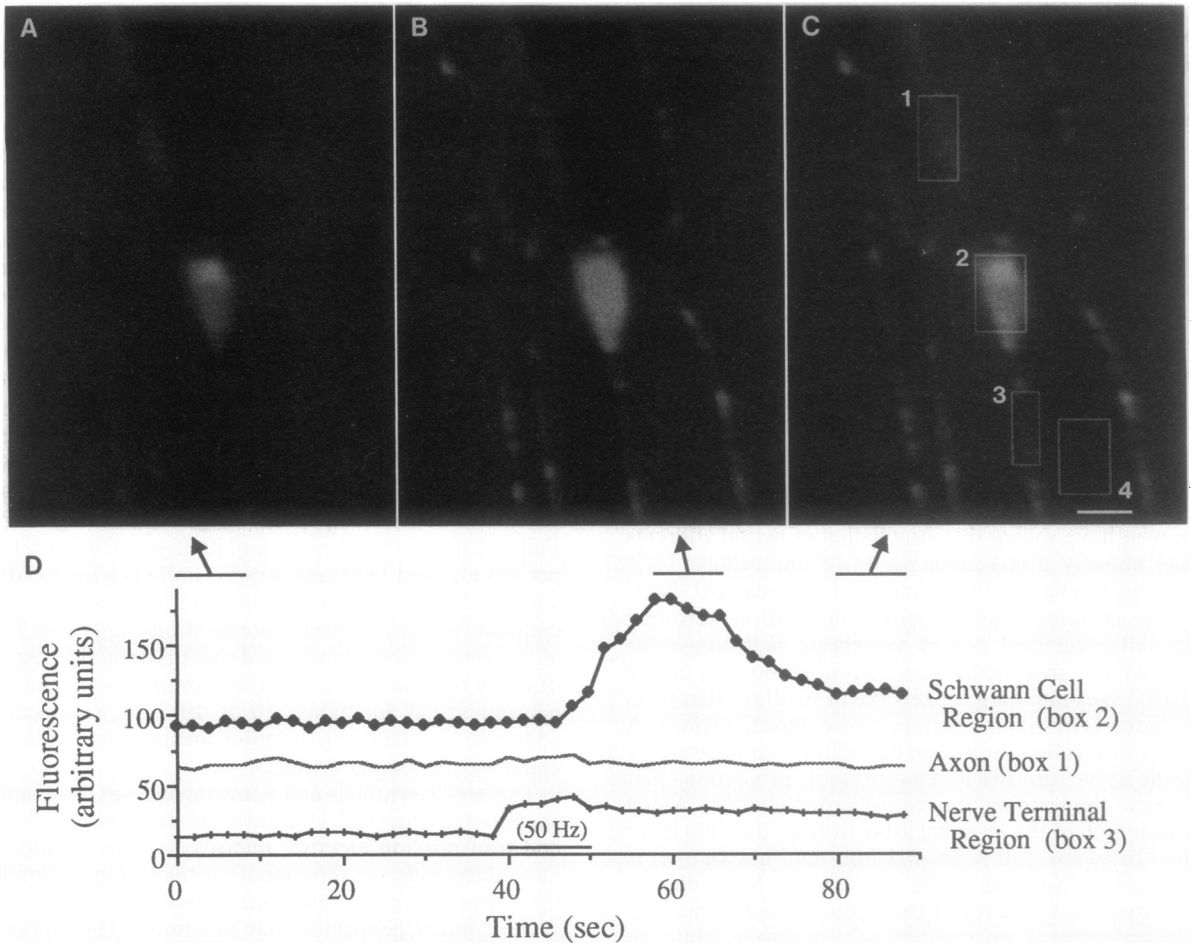

FIG. 1. Effect of motor-nerve stimulation on intracellular Ca^{2+} levels in a terminal Schwann cell of an innervated sheath preparation. Fluorescence images were obtained by averaging groups of five consecutive images, as indicated by the arrows in *D*. (*A*) Resting fluorescence. (*B*) Fluorescence during peak Schwann cell response. (*C*) Fluorescence during recovery. Box 1 contains the axon and its associated, myelinating Schwann cell. Box 2 is dominated by a large Schwann cell soma, although it also contains nerve terminal. Although box 3 contains a thin process from the terminal Schwann cell, this subarea is dominated by nerve terminal (see text). Box 4 contains a region devoid of cells used to measure the background fluorescence. (*D*) Graph of mean fluorescences of the myelinated axon, the Schwann cell soma region, and the nerve-terminal region vs. time. Mean background fluorescence was subtracted before graphing. Timing and frequency of electrical stimulation to the motor nerve are indicated. (Bar = 10 μm.)

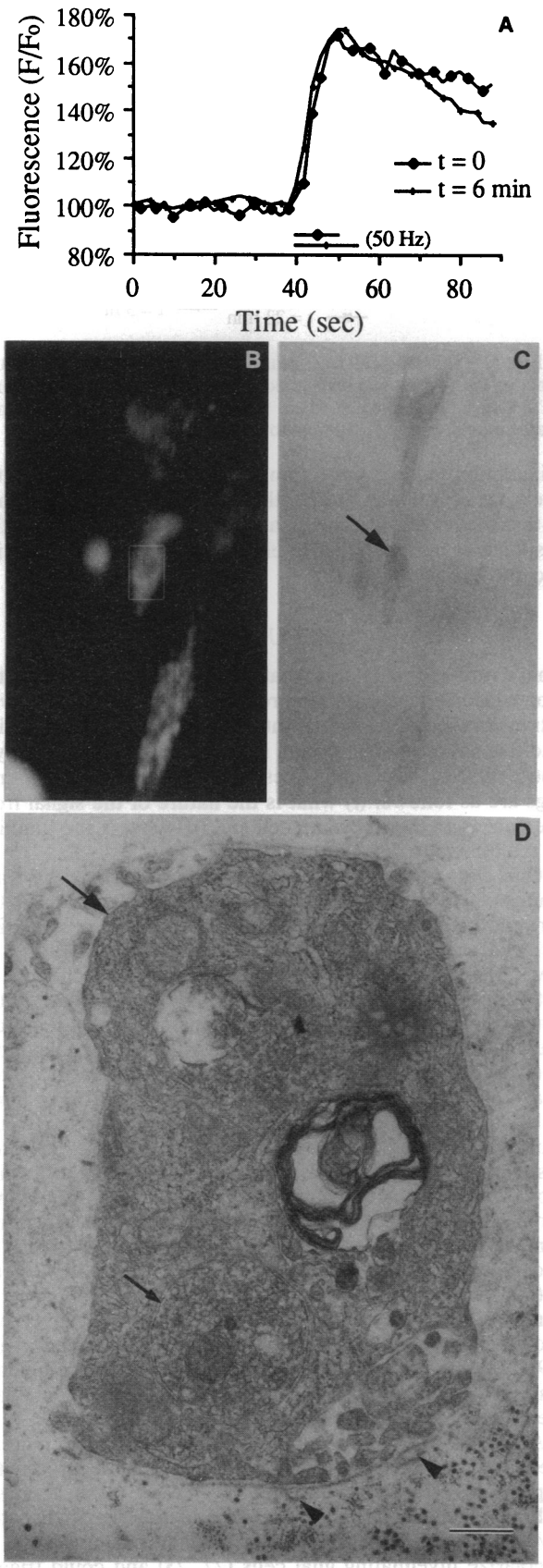

FIG. 2. Identification by electron microscopy of a cell that exhibited a Ca^{2+} transient. (*A*) Relative fluorescence of the subarea indicated in the box in *B* is graphed vs. time during each of two stimulation trials. The motor nerve was stimulated at 50 Hz at the times indicated by horizontal bars. The relative start time for each stimulation trial is indicated. (*B*) Whole-mount fluorescence micrograph of a cell that exhibited a Ca^{2+} transient in an innervated sheath preparation; cell of interest is located within box. (*C*) Same field as in *B* relocated by transmitted light microscopy after fixation and embedding. Arrow indicates cell of interest. (*D*) Electron micrograph of a cross-section through the cell soma (large arrow). A vesicle-filled nerve terminal is indicated by the small arrow, and fingers of basal lamina that previously occupied junctional folds are indicated by arrowheads. (Bar = 8 μm in *B*; 10 μm in *C*; and 0.2 μm in *D*.)

such a Ca^{2+} transient in an innervated sheath preparation is illustrated in Fig. 1, where the increase in free Ca^{2+} is indicated by an increase in brightness of the fluorescence image. To examine the timing of the Ca^{2+} transient, the mean fluorescence of the subareas indicated in Fig. 1*C* was graphed vs. time (Fig. 1*D*). The resting fluorescence (before stimulation) was stable, and stimulation of the motor nerve did not affect the fluorescence levels of the background (box 4) or of the axon/myelinating Schwann cell (box 1). Under our recording regime, the fluorescence of the nerve-terminal region (box 3) increased simultaneously with stimulus onset and did not return to baseline during the recorded recovery period (40 sec). These kinetics are consistent with reports of residual calcium within motor nerve terminals after tetanic stimulation (9, 10). After a latent period (≈8 sec in this example) fluorescence of the terminal Schwann cell soma region increased (box 2). The rising phase of this particular transient was fairly slow (several seconds), and the response reached a peak fluorescence increase of 1.6-fold ≈20 sec after onset of the stimulation.

The latency and magnitude of the Schwann cell response varied significantly for different terminal Schwann cells; the latency ranged from 2 sec to 20 sec, and the magnitude ranged from 1.3- to 7-fold (21 cells, 35 observations). Occasionally, an exceptionally bright nerve-terminal response generated a detectable signal within a "Schwann cell-dominated region"—a small fast transient preceding the larger, slower response. In such cases, subareas were selected over portions of the Schwann cell soma that excluded the nerve terminal. We were unable to detect any fluorescence increases in nerve-terminal-dominated regions (for example, Fig. 1*C*, box 3) that had latencies similar to those of the Schwann cell soma regions. Possible explanations for this include the following: (*i*) the Schwann cell processes in the nerve-terminal regions did not exhibit Ca^{2+} responses, (*ii*) Ca^{2+} responses occurred in these processes but with different kinetics, or (*iii*) the Ca^{2+} responses in these thin Schwann cell processes were obscured by larger responses in the nerve terminal.

The cells that exhibited Ca^{2+} transients in this study were classified as terminal Schwann cells based on their morphology as seen by Nomarski and fluorescence imaging. However, examination by light microscopy could not rule out the possibility that these presumed Schwann cells might, instead, be stray satellite cells that might have survived the irradiation protocol and migrated to a synaptic site or abnormal enlargements of the nerve terminal in these innervated sheath preparations. To verify that the responsive cells were indeed Schwann cells, two of the cells that exhibited Ca^{2+} transients upon motor-nerve stimulation were relocated in electron micrographs. Fig. 2*A* is a graph of two sequential Ca^{2+} transients from one of these cells (Fig. 2*B*, boxed cell). The same cell was relocated in the whole-mount preparation after fixation (Fig. 2*C*, arrow). An electron micrograph of a cross-section through the soma of the cell shown in Fig. 2 *B* and *C* is shown in Fig. 2*D*. The vesicle-filled nerve terminal (small arrow) and the basal lamina fingers (arrowheads) identify this as a synaptic site (11). The cell that exhibited the Ca^{2+} transients (large arrow) has enveloped the nerve terminal in this section; its intimate association with the terminal

inside of a basal lamina sheath clearly identifies this cell as a terminal Schwann cell.

Repeated stimulation usually induced repeated Ca^{2+} responses from individual Schwann cells (11 of 13). Fig. 3 illustrates variations in responses to repeated neuronal stimulation. Each graph shows the fluorescence of a single Schwann cell soma relative to its resting fluorescence before each stimulus, during five stimulation trials. Intervals between trials are indicated in the key. The magnitude of the Ca^{2+} transient within a given Schwann cell usually decreased with repeated stimulations (Fig. 3 *A* and *B*; Fig. 4), although the first transient was not always the largest (Figs. 3*B* and 4). Individual Schwann cells showed a large variation in latencies during multiple stimulation trials (see Figs. 3*A* and 4). Finally, two Schwann cells imaged simultaneously at the same neuromuscular junction (compare Fig. 3 *A* and *B*) can respond to the same stimuli with different timing and different relative magnitudes. The Schwann cell in Fig. 3*A* responded earlier than the one in Fig. 3*B*, and the first stimulus produced the largest response from the Schwann cell in Fig. 3*A*, whereas the response to the second stimulus was largest in Fig. 3*B*.

To exclude the possibility that the Schwann cell Ca^{2+} transients are a peculiarity of this innervated sheath preparation, we examined Ca^{2+} levels at intact neuromuscular junctions labeled the same way. *d*-Tubocurare was present during stimulation to prevent muscle contraction. Fig. 4 graphs the mean fluorescence of a terminal Schwann cell at an intact junction during repeated stimulation of the motor nerve. Again the latency and the magnitude of the Schwann cell response were highly variable. The responses at intact junctions (n = 4) were qualitatively similar to the responses seen in our innervated sheaths. The decay of the response in intact muscles may be more rapid (for example, compare Figs. 3*A* and 4), but given the large variability in the Schwann cell responses, a larger sample size would be needed for quantitative analysis. Finally, the observation that neuronal

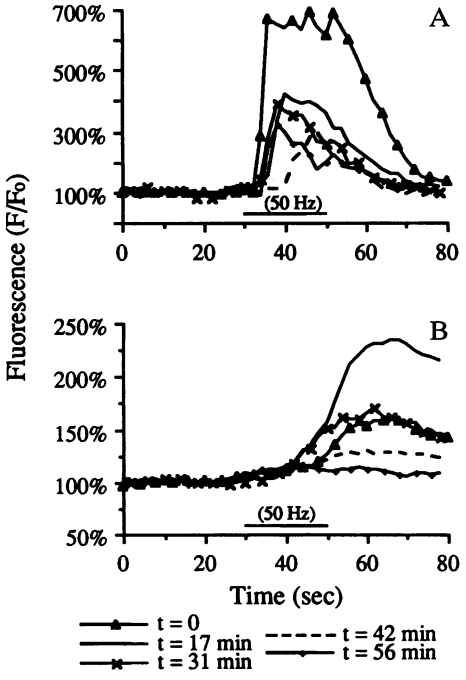

FIG. 3. Schwann cell Ca^{2+} transients induced by repetitive stimulation of motor nerve. The change in fluorescence induced by each of five stimulation trials for two individual Schwann cells at a single nerve-terminal arborization is graphed vs. time as in Fig. 2*A*. The motor nerve was stimulated at 50 Hz over the time indicated by the horizontal bar.

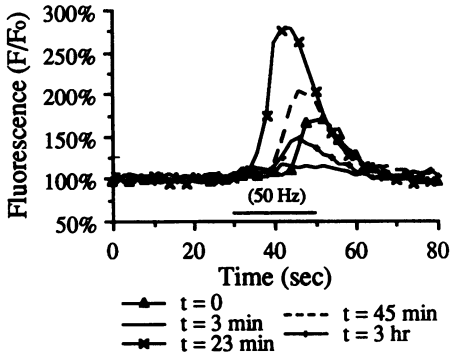

FIG. 4. Schwann cell Ca^{2+} transients at an intact neuromuscular junction in the presence of *d*-tubocurare. The change in fluorescence of a single Schwann cell at an intact neuromuscular junction is graphed as in Fig. 2*A*. Stimulation frequency was 50 Hz.

stimulation induces Ca^{2+} transients in Schwann cells in the presence of *d*-tubocurare, both in intact muscles (Fig. 4) and in the innervated sheaths (data not shown), indicates that this response is not mediated solely by a nicotinic acetylcholine receptor.

DISCUSSION

These studies demonstrate that terminal Schwann cells at the frog neuromuscular junction respond to neural activity with a transient increase in their intracellular Ca^{2+} concentration and that this response occurs in the absence of the postsynaptic muscle. Two major questions arising from these findings are as follows: (*i*) what is the nature of the signal from the neuron to the Schwann cell and (*ii*) what is the function of the Schwann cell-Ca^{2+} response.

One clue as to the nature of the signal is that the Ca^{2+} transients in our system are specific to the synapse: the terminal Schwann cells respond, and the myelinating Schwann cells along the axon do not (see Fig. 1*C*, box 1). Thus, the signal may be a molecule released specifically by active motor-nerve terminals. An obvious candidate is the neurotransmitter acetylcholine, by analogy to studies from the central nervous system, suggesting that the excitatory neurotransmitter glutamate induces Ca^{2+} signals in central glial cells (12–15). If the neuronal signal to the terminal Schwann cell is acetylcholine, however, the receptor would most likely be of the muscarinic type, because the Ca^{2+} response occurs in the presence of curare (see Fig. 4), which blocks nicotinic acetylcholine receptors. Other candidates for a synapse-specific signal include ATP and calcitonin gene-related peptide (CGRP). In skeletal muscle, both ATP and calcitonin gene-related peptide are found in vesicles within motor-nerve terminals and are released upon nerve stimulation (16–18). Low concentrations of ATP have been shown to stimulate Ca^{2+} transients in cultures of central glia (19, 20). Pharmacological manipulations may elucidate whether one or more of these compounds do, indeed, mediate the neurally induced Schwann cell response.

Alternatively, the Schwann cell Ca^{2+} transients could be mediated by a nonsynapse-specific signal, such as an activity-dependent efflux of neuronal K^+ (21), if the terminal Schwann cells were more sensitive to the signal than the myelinating Schwann cells. K^+ efflux has been shown to depolarize myelinating glial cells (22, 23) and could trigger glial Ca^{2+} transients if the Schwann cells have voltage-gated Ca^{2+} channels. It has recently been reported (24) that long, rapid stimulation of frog sciatic nerve generates Ca^{2+} transients in myelinating Schwann cells and it may be that the less vigorous stimulation paradigm used in our experiments is simply insufficient to generate detectable Ca^{2+} transients in

the myelinating Schwann cells. Thus, it is possible that the synapse specificity seen in our system arises either from a greater sensitivity to K^+-induced depolarization of terminal vs. myelinating Schwann cells or from a larger increase in external $[K^+]$ in the terminal region compared with the axon.

At this point in our studies, we can only speculate as to possible functions of the Schwann cell Ca^{2+} transients. At the frog neuromuscular junction, the synaptic delay between the depolarization of the nerve terminal and that of the muscle fiber is <1 msec (25). We found that the latency between the Ca^{2+} transient within the nerve terminal and the Ca^{2+} transient within the terminal Schwann cell was relatively long (2–20 sec). Thus, the Ca^{2+} transient within the Schwann cell is too slow to be involved in the initial transmission between the nerve terminal and the muscle fiber. It may be that the Schwann cell Ca^{2+} signals are involved with the development and/or maintenance of normal terminal/Schwann cell relations. For example, the absence of the Schwann cell Ca^{2+} transient could signal the Schwann cell to exhibit the phagocytic activity seen at denervated junctions (26, 27). Alternatively, these Ca^{2+} transients could mediate some modulatory activity of the Schwann cells on synaptic function. Intracellular Ca^{2+} signals commonly regulate cellular function (28), and neuromodulatory roles have been previously postulated for other glial cells (2).

The observations reported here reinforce earlier suggestions (2, 29, 30) that a full understanding of synaptic transmission may not be achieved until glial cells are recognized as active components of the synapse. In light of this, we propose designating the Ca^{2+} response of the terminal Schwann cell as a "perisynaptic response," parallel to, but distinct from, the postsynaptic response of the muscle. The functional role of such a perisynaptic response in synaptic transmission remains as a subject for future studies. The amphibian neuromuscular junction should prove to be an ideal system for assessing the function of glial Ca^{2+} signals, given the ease with which identified pre- and postsynaptic components can be manipulated and the extensive literature detailing the morphology, physiology, and pharmacology of this junction.

We thank Dr. Robert Galambos, Dr. Michael Dailey, and Dwight Bergles for comments on the manuscript and helpful discussions. The work was supported by a National Institute of Mental Health Silvio Conte Center for Neuroscience Research Grant (MH48108), by a grant from the National Institute of Neurological Diseases and Stroke (NS 28587), a gift from the G. Harold and Leila Y. Mathers Charitable Foundation, and a National Research Service Award from the National Institute of Neurological Disorders and Stroke (NS08918 to N.E.R.).

1. Kuffler, S. W., Nicholls, J. G. & Martin, A. R. (1984) *From Neuron to Brain: A Cellular Approach to the Function of the Nervous System* (Sinauer, Sunderland).
2. Barres, B. A. (1991) *J. Neurosci.* **11**, 3685–3694.
3. Dani, J. W., Chernjavski, A. & Smith, S. J. (1992) *Neuron* **8**, 429–440.
4. McMahan, U. J., Spitzer, N. C. & Peper, K. (1972) *Proc. R. Soc. London Ser. B* **181**, 421–430.
5. Yao, Y.-M. M. (1988) in *Current Issues in Neural Regeneration Research*, eds. Reier, P. J., Bunge, R. P. & Seil, F. J. (Liss, New York), pp. 167–178.
6. Jahromi, B., Robitaille, R. & Charlton, M. P. (1991) *Soc. Neurosci. Abstr.* **17**, 900.
7. Valdiosera, R., Clausen, C. & Eisenberg, R. S. (1974) *J. Gen. Physiol.* **63**, 460–491.
8. McMahan, U. J. & Slater, C. R. (1984) *J. Cell Biol.* **98**, 1453–1473.
9. Katz, B. & Miledi, R. (1968) *J. Physiol. (London)* **195**, 481–492.
10. Delaney, K. R., Zucker, R. S. & Tank, D. W. (1989) *J. Neurosci.* **9**, 3558–3567.
11. Sanes, J. R., Marshall, L. M. & McMahan, U. J. (1978) *J. Cell Biol.* **78**, 176–198.
12. Enkvist, M. O. K., Holopainen, I. & Akerman, K. E. O. (1989) *Glia* **2**, 397–402.
13. Cornell-Bell, A. H., Finkbeiner, S. M., Cooper, M. S. & Smith, S. J. (1990) *Science* **247**, 470–473.
14. Jensen, A. M. & Chiu, S. Y. (1990) *J. Neurosci.* **10**, 1165–1175.
15. Charles, A. C., Merrill, J. E., Dirksen, E. R. & Sanderson, M. J. (1991) *Neuron* **6**, 983–992.
16. Silinsky, E. M. & Hubbard, J. I. (1973) *Nature (London)* **243**, 404–405.
17. Matteoli, M., Haimann, C., Torri-Tarelli, F., Polak, J. M., Ceccarelli, B. & De Camilli, P. (1988) *Proc. Natl. Acad. Sci. USA* **85**, 7366–7370.
18. Uchida, S., Yamamoto, H., Iio, S., Matsumoto, N., Wang, X. B., Yonehara, N., Imai, Y., Inoki, R. & Yoshida, H. (1990) *J. Neurochem.* **54**, 1000–1003.
19. Neary, J. T., van Breeman, C., Forster, E., Norenberg, L. O. B. & Norenberg, M. D. (1988) *Biochem. Biophys. Res. Commun.* **157**, 1410–1416.
20. Pearce, B., Murphy, S., Jeremy, J., Morrow, C. & Dandona, P. (1989) *J. Neurochem.* **52**, 971–977.
21. Katz, B. & Miledi, R. (1982) *Proc. R. Soc. London Ser. B* **216**, 497–507.
22. Orkand, R. K., Nicholls, J. G. & Kuffler, S. W. (1966) *J. Neurophysiol.* **29**, 789–806.
23. Lev-Ram, V. & Grinvald, A. (1986) *Proc. Natl. Acad. Sci. USA* **83**, 6651–6655.
24. Lev-Ram, V. & Ellisman, M. H. (1991) *Soc. Neurosci. Abstr.* **17**, 1519.
25. Katz, B. & Miledi, R. (1964) *Proc. R. Soc. London Ser. B* **161**, 483–495.
26. Birks, R., Katz, B. & Miledi, R. (1960) *J. Physiol. (London)* **150**, 145–168.
27. Miledi, R. & Slater, C. R. (1970) *J. Physiol. (London)* **207**, 507–528.
28. Stryer, L. (1988) *Biochemistry* (Freeman, New York).
29. Galambos, R. (1961) *Proc. Natl. Acad. Sci. USA* **47**, 129–136.
30. Teichberg, V. I. (1991) *FASEB J.* **5**, 3086–3091.